

1 **APPENDIX I. SUPPLEMENTAL MATERIAL**

2

3 **Diminished force production and mitochondrial respiratory deficits are strain-**
4 **dependent myopathies of subacute limb ischemia.**

5

6 *Short Title:* Strain dependent mitochondrial dysfunction in subacute ischemia

7

8 Cameron A. Schmidt^{1,2}, Terence E. Ryan^{1,2}, Chien-Te Lin^{1,2}, Melissa M.R. Inigo^{1,2}, Tom
9 D. Green^{1,2}, Jeffrey J. Brault³, Espen E. Spangenburg^{1,2}, & Joseph M. McClung^{1,2}

10

11 ¹Department of Physiology, ²Diabetes and Obesity Institute, Brody School of Medicine,

12 ³Department of Kinesiology, East Carolina University, Greenville, NC.

13

14 Correspondence should be addressed to J.M.M.: Diabetes and Obesity Institute, Office
15 #4109, Mail Stop 743, East Carolina Heart Institute, Brody School of Medicine at East
16 Carolina University, 115 Heart Drive, Greenville, NC 27834-4354. Tel: 252-737-5034
17 (office); Fax: 252-744-3460; email: mcclungj@ecu.edu

18

19

20

21

22

23

24 **Materials and Methods**

25 *Animals.* Experiments were conducted on adult (12-16 week) C57BL/6J (N=33) or
26 BALB/cJ (N=36) mice. All work was approved by the Institutional Review Committee
27 of East Carolina University. Animal care was in compliance with the Guide for the Care
28 and Use of Laboratory Animals, Institute of Laboratory Animal Resources, Commission
29 on Life Sciences, National Research Council. Washington: National Academy Press,
30 1996. Sub-acute ischemia was performed as previously described¹, with the following
31 modifications. Mice were anesthetized by intraperitoneal injection of ketamine (90
32 mg/kg) and xylazine (10 mg/kg) and an ameroid constrictor (AC; 0.25 mm internal
33 diameter; Research Instruments SW, Escondido, Calif) was placed on the femoral artery
34 immediately distal to the lateral circumflex femoral artery and proximal to the origin of
35 the superficial caudal epigastric artery. The inferior epigastric, lateral circumflex, and
36 superficial epigastric artery branches of the femoral artery were left intact to preserve
37 collateral perfusion to the limb. The cardiotoxin model (CTX) of mouse muscle
38 regeneration was performed as previously described² using 20µL I.M. injections of 5µM
39 *Naja nigricollis* venom into the tibialis anterior, medial and lateral heads of the
40 gastrocnemius with a 27 gauge needle under anesthesia. An equivalent volume sham
41 injection of 1X phosphate buffered saline (PBS) was administered to the muscles of the
42 contralateral hindlimb. Because CTX was not directly injected into the EDL, but EDL
43 muscles were used for various measurements in this study, a test animal (C57BL/6) was
44 sacrificed 24hrs following TA injection of CTX and the EDL muscle was isolated and
45 histologically stained to confirm that the extent of injury was identical to the TA muscle.

46 *Assessment of limb perfusion and tissue SO₂.* Limb blood flow was measured using laser
47 Doppler perfusion (LDPI) imaging as previously described¹ with the following
48 modifications. Imaging was performed at a 4ms/pixel scan rate on animals placed on a
49 37C warming pad in the prone position under ketamine/xylazine anesthesia, using a Moor
50 Instruments LDI2-High Resolution (830 nM) System (Moor, Axminster, UK) up to 28
51 days post intervention. Hindlimb hair was removed with depilatory cream 24 hours prior
52 to initial scanning and hair was removed with a microshaver at all other timepoints.
53 Images were analyzed with the MoorLDI Image Review software. Tissue oxygen
54 saturation (SO₂) was assessed at the aforementioned timepoints using a Moor VMS-OXY
55 white light spectrometer with a CPT-300 optical probe. SO₂ measurements were taken
56 immediately following LDPI imaging for each animal to minimize positional variation.
57 The optical probe was placed on the ventro-medial region of the paw (SLI, CTX), as well
58 as the TA and lateral head of the gastrocnemius muscle (CTX). Stable signal was
59 collected for ten seconds. Data were analyzed using the Moor VMS review software.
60 Results for both analyses were expressed as a ratio of the treated limb to the untreated
61 (SLI) or sham injected (CTX) contralateral limb.

62 *Primary Antibodies and histological stains.* The following commercial antibodies were
63 used: CD31 (AbdSerotec MCA-1364), dystrophin (Thermo Scientific RB-9024), total
64 oxphos (AbCam 110413), MHC type I (BA-D5, DHSB), MHC type IIa (SC-71, DHSB),
65 MHC type IIb (BF-F3, DHSB), CD11b (AbCam 52478). DAPI mounting medium
66 (VECTOR Laboratories, H-1200) was also used. Histological stains were obtained from
67 Sigma-Aldrich: Mayer's hematoxylin, F8775; Direct red 80 (sirius red), MHS16; Picric
68 acid, P6744; Weigert's hematoxylin, HT1079.

69 *Immunofluorescence (IF) and Histology.* 8- μ m-thick (12- μ m-thick for oil red o)
70 transverse sections from tibialis anterior frozen in liquid nitrogen cooled isopentane in
71 optimum cutting temperature medium (OCT) were cut using a Leica 3050S cryotome and
72 collected on charged slides for staining. For morphological analyses, standard methods
73 for hematoxylin and eosin (H&E), oil red o (intramuscular lipids), and picrosirius red
74 (collagen) histological staining were performed. Analysis of muscle regeneration was
75 performed on whole image transverse sections compiled of 40X tiled H&E images using
76 an Aperio CS2 digital slide analyzer (Leica Biosystems) and the aperio imagescope
77 software (v12.0, default settings). Sections were segregated into regions of interest (ROI)
78 by morphology representative of tissue regeneration. ROIs were traced by a blinded
79 investigator using the following categories: regenerating, intact myofibers with peripheral
80 nuclei and/or small basophilic myofibers with centralized nuclei and low to moderate
81 granulation tissue; non-regenerating, granulation tissue with few to no basophilic
82 myofibers and/or anucleate necrotic fibers. Muscle tissue morphology was presented as a
83 % of the total muscle area including intact fibers and fascicular structure, the total
84 number of myofibers, and the total number of myofibers with centralized nuclei. Analysis
85 of lipid content was performed on 12- μ m sections rinsed in 60% ethanol and stained in
86 oil red o (3 volumes of 1g/100mL oil red o in 99% isopropyl alcohol, in two volumes of
87 1% dextrin) for 20 mins. Slides were then counterstained in mayer's hematoxylin and
88 washed prior to coverslipping with a glycerol gelatin mounting medium at 37°C. 10X
89 brightfield images were obtained and lipid positive staining was quantified by a blinded
90 investigator in Imagej (NIH, v1.49) by thresholding hue, saturation, and brightness
91 colorspace and measuring the percent area of lipid positive stain within the field of view.

92 Upper and lower threshold bounds were kept constant among all images analyzed.
93 Collagen deposition was quantified by picrosirius red. Slides were allowed to come to
94 room temperature and stained in weigert's hematoxylin soln for 10 mins and were then
95 rinsed in circulating tap water for 10 mins. Slides were then stained in a working soln of
96 picrosirius red (sirius red .5g/500mL, saturated picric acid 500mL) for one hour and
97 washed in acidified water before dehydration in ethanol, clearance in xylene, and
98 mounting using glycerol gelatin at 37°C. 10X images were taken on an Olympus BX51-P
99 polarized light microscope and collagen deposition was quantified by a blinded
100 investigator in Imagej (NIH, v1.49) by thresholding hue, saturation, and brightness
101 colorspace and measuring the percent area of the field of view occupied by each of two
102 birefringent hue categories: red/orange and yellow/green. Upper and lower bounds for
103 thresholding were kept constant among all images analyzed. To assess the relative
104 distributions of muscle interstitial cells with lipid positive inclusions, transverse sections
105 were prepared as described above with the exception of fixation. The unfixed sections
106 were immunostained for dystrophin as described above for use as a counterstain. Sections
107 were then stained with 1ug/mL BODIPY 493/503 (ThermoFisher) in 1X PBS diluent for
108 30 mins. Slides were then mounted in Vectashield hard mount medium with DAPI and
109 imaged as described above. Image quantification was performed on representative 10X
110 images by a blinded investigator using ImageJ (NIH, v1.49) by decomposing the images
111 into RBG colorspace, setting appropriate standard threshold value limits, and measuring
112 the percent area of BODIPY positive stain within each image.

113 Vascular density and morphology IF was performed as previously described^{1,3}. Briefly,
114 transverse sections were allowed to come to room temperature and were

115 fixed/permeabilized with ice-cold 1:1 acetone/methanol for 10 minutes at 4C. Fixed
116 sections were allowed to air dry for 5 minutes at room temperature (RT) and rehydrated
117 in 1X PBS before blocking in 5% normal goat serum (Sigma) in 1X PBS at RT for 45
118 min. Slides were then incubated overnight at 4C in a primary antibody solution. Slides
119 were washed three times in 1X PBS at RT and incubated for 1 hour at RT in the dark in a
120 secondary solution containing a 1:250 dilution of Alexa Fluor 488, or 647 conjugated
121 secondary antibodies in blocking solution. Sections were washed in the dark three times
122 for 5 minutes each with 1X PBS at RT, and coverslips were mounted using Vectashield
123 HardSet Mounting Medium with DAPI (Vector Labs H- 1500). Images were captured
124 using a Life Technologies Evos auto FL wide field fluorescence microscope (Thermo
125 Fisher) and analyzed by a blinded investigator using ImageJ (NIH, v1.49). Five 20X
126 images were captured per section from similar topographical regions. Images were
127 decomposed to red-blue-green (RBG) composites, thresholded using the same upper and
128 lower bounds for all images analyzed, and presented as the mean percent CD31⁺ area per
129 20X field of view. These measurements were interpreted as being proportional to the
130 density of the capillary bed in the muscle. Myofiber cross sectional areas were quantified
131 by thresholding dystrophin positive signal until segmentation was achieved and analyzing
132 the area of each complete fiber in the field of view using ImageJ (NIH, v1.49). Myofiber
133 areas were measured in microns squared (μm^2) and presented as a ratio of the insulted
134 limb (L) to the contralateral control limb (R). Muscle fiber type IF staining was
135 performed as previously described⁴. Briefly, transverse sections were allowed to come to
136 room temperature and were fixed/permeabilized with ice-cold 1:1 acetone/methanol for
137 10 minutes at 4C. Fixed sections were allowed to air dry for 5 minutes at room

138 temperature (RT) and rehydrated in 1X PBS before blocking in 5% normal goat serum
139 (Sigma) in 1X PBS at RT for 45 min. Slides were then incubated overnight at 4C in a
140 primary antibody solution including antigens directed at dystrophin, MHC type I, MHC
141 type IIa, or MHC type IIb (MHC type IIx would be unstained). Slides were washed three
142 times in 1X PBS at RT and incubated for 1 hour at RT in the dark in a secondary solution
143 containing a 1:250 dilution of Alexa Fluor secondary antibodies in blocking solution.
144 Sections were washed in the dark three times for 5 minutes each with 1X PBS at RT, and
145 coverslips were mounted using Vectashield HardSet Mounting Medium with DAPI
146 (Vector Labs H- 1500). Images were captured using a Life Technologies Evos auto FL
147 wide field fluorescence microscope (Thermo Fisher) and analyzed by a blinded
148 investigator using ImageJ (NIH, v1.49). Four 10X images were captured per section from
149 similar topographical regions using a Life Technologies Evos auto FL wide field
150 fluorescence microscope (Thermo Fisher) and analyzed by a blinded investigator using
151 ImageJ (NIH, v1.49). Data are presented as the percentage of total myofibers of each
152 fiber type (MHC type I, MHC type IIa, or MHC type IIb).

153 *Immunoblotting.* Extensor digitorum longus (EDL) muscles were isolated and snap
154 frozen in liquid nitrogen. Frozen muscles were homogenized in ice-cold RIPA Lysis
155 buffer containing protease and phosphatase inhibitors. Protein concentrations were
156 determined using a BCA protein assay (Pierce, ThermoFisher #23225). Proteins were
157 then separated using an SDS-Page gel (Mini-Protean TGX, Bio-Rad #4561093) with
158 50ug total protein loaded per well. Blots were visualized with chemiluminescence using
159 standard film procedures.

160 *Preparation of isolated skeletal muscle mitochondria.* Skeletal muscle mitochondria were
161 isolated from the plantar flexor (i.e. gastrocnemius, plantaris, and soleus) muscles of both
162 control (R) and injured (L) hindlimbs as previously described⁵. Muscle was pooled from
163 two animals to ensure sufficient mitochondrial yield was obtained. Following dissection,
164 muscle was washed in mitochondrial isolation medium (MIM) containing 300mM
165 sucrose, 10mM HEPES, and 1mM EGTA. Muscle was minced on ice using fine tipped
166 scissors for five minutes. Muscle was then washed and resuspended in MIM + 1mg/mL
167 bovine serum albumin (MIM+BSA) and homogenized on ice using a Teflon pestle and
168 Wheaton overhead stirrer. The homogenate was centrifuged at 800xg to pellet non-
169 mitochondrial myofibrillar proteins, nuclei, and other cellular components. The
170 supernatant was transferred to a pre-chilled oakridge tube and then centrifuged at
171 12,000xg to pellet mitochondria. The mitochondrial pellet was washed and resuspended
172 in 100µl of MIM and stored on ice until analysis (less than 1 hr). Mitochondrial protein
173 content was determined by BCA protein assay (Pierce).

174 *Mitochondrial respiration measurements.* High-resolution O₂ consumption measurements
175 were conducted at 37°C in buffer Z (105 mM K-MES, 30 mM KCl, 1 mM EGTA, 10
176 mM K₂HPO₄, 5 mM MgCl₂·6H₂O, 0.5 mg/ml BSA, pH 7.1), supplemented with creatine
177 monohydrate (20 mM), using the OROBOROS O2K Oxygraph. A substrate inhibitor
178 titration protocol was performed as follows: 2mM Malate + 10mM Glutamate (State 2
179 respiration), followed by the addition of 4mM ADP to initiate State 3 respiration
180 supported by Complex I substrates, convergent electron flow through complexes I and II
181 was initiated with the addition of 10mM Succinate, 10µM Rotenone was subsequently
182 added to inhibit Complex I, followed by 10µM Cytochrome C to test the integrity of the

183 mitochondrial membrane, Complex IV supported respiration was examined using the
184 electron donor N,N,N',N'-tetramethyl-p-phenylenediamine (TMPD) at 0.5mM in the
185 presence of 2mM Ascorbate (to limit auto-oxidation of TMPD) and 5 μ M of Antimycin A
186 (to prevent reverse electron flow through Complex III), finally, uncoupled respiration
187 was assessed with the addition of 0.5 μ M Carbonyl cyanide-4-
188 (trifluoromethoxy)phenylhydrazone (FCCP). The rate of respiration was expressed as
189 pmol/s/mg mitochondrial protein.

190 *Preparation of permeabilized muscle fibers.* During sacrifice, a portion of the red
191 gastrocnemius muscle was removed and immediately placed in ice-cold buffer X (50 mM
192 K-MES, 7.23 mM K₂EGTA, 2.77 mM CaK₂EGTA, 20 mM imidazole, 20 mM taurine,
193 5.7 mM ATP, 14.3 mM phosphocreatine, and 6.56 mM MgCl₂-6H₂O, pH 7.1) for
194 preparation of permeabilized fiber bundles (PmFBs) as previously described⁶. Fiber
195 bundles were separated along their longitudinal axis using needle-tipped forceps under
196 magnification (MX6 Stereoscope, Leica Microsystems, Buffalo Grove, IL, USA),
197 permeabilized with saponin (30 μ g/ml) for 30 minutes at 4°C, and then washed in cold
198 buffer Z (105 mM K-MES, 30 mM KCl, 1 mM EGTA, 10 mM K₂HPO₄, 5 mM MgCl₂-
199 6H₂O, 0.5 mg/ml BSA, pH 7.4) for approx. 20 minutes until analysis. At the conclusion
200 of each experiment, PmFBs were washed in double-distilled H₂O to remove salts, freeze-
201 dried (Labconco), and weighed. Typical fiber bundle sizes were 0.2-0.4 mg dry weight.

202 *Isolated myofiber respiration measurements.* High-resolution O₂ consumption
203 measurements were conducted at 37°C in buffer Z (105 mM K-MES, 30 mM KCl, 1 mM
204 EGTA, 10 mM K₂HPO₄, 5 mM MgCl₂6H₂O, 0.5 mg/ml BSA, pH 7.1), supplemented
205 with creatine monohydrate (20 mM), using the OROBOROS O2K Oxygraph. An

206 abbreviated protocol similar to that used for isolated mitochondria was performed,
207 described as follows: 2mM Malate + 10mM Glutamate (State 2 respiration), followed by
208 the addition of 4mM ADP to initiate State 3 respiration supported by Complex I
209 substrates, convergent electron flow was next initiated with the addition of 10mM
210 Succinate, 10 μ M Rotenone was subsequently added to inhibit Complex I, followed by
211 10 μ M Cytochrome C to test the integrity of the mitochondrial membrane. The rate of
212 respiration was normalized to the myofiber dry weight and expressed as pmol/s/mg dry
213 weight.

214 *Mitochondrial calcium retention capacity.* To determine susceptibility to opening of the
215 mitochondrial permeability transition pore (mPTP), preparations of isolated mitochondria
216 were exposed to progressively increasing calcium load in the presence of (in mM): 5
217 malate, 10 glutamate, 0.02 ADP. Changes in extramitochondrial calcium concentration
218 were monitored fluorometrically using Calcium Green (1 μ M, excitation/emission
219 506/532 nm, Invitrogen) per the manufacturer's instructions. All experiments were run at
220 37 °C in Buffer Z containing 2 U/ml hexokinase and 5 mM 2-deoxyglucose (to clamp
221 respiration).

222 *Citrate synthase activity assays.* Activity assays were performed using a citrate synthase
223 activity assay kit (Sigma). Briefly, extensor digitorum longus (EDL) muscles were
224 isolated and snap frozen in liquid nitrogen. Frozen muscles were homogenized in ice-cold
225 Lysis buffer. Protein concentrations were determined using a BCA protein assay (Pierce,
226 ThermoFisher #23225). Activity assays were performed in assay buffer containing (in
227 mM): 100 Tris, 1 EDTA, 1 EGTA, 10 DTNB (Sigma: D8130), and 30 Acetyl CoA at pH
228 8.35. All samples were measured in triplicate and the average absorbance was used in

229 final calculations of activity. Background absorbance was measured prior to addition of
230 10mM oxoloacetate (Sigma: 04126) and final activity rates were corrected for those
231 values.

232 *Muscle contractile force measurements.* Contractile force was performed as previously
233 described⁷. In brief, single EDL muscles were surgically excised with ligatures at each
234 tendon (5–0 silk suture) and mounted in a bath between a fixed post and force transducer
235 (Aurora 300B-LR) operated in isometric mode. The muscle was maintained in modified
236 Krebs's buffer solution (PSS; pH 7.2) containing (in mM) 115 NaCl, 2.5 KCl, 1.8 CaCl₂,
237 2.15 Na₂HPO₄, .85 NaH₂PO₄, and maintained at 25°C under aeration with 95% O₂–5%
238 CO₂ throughout the experiment. Resting tension and muscle length were iteratively
239 adjusted for each muscle to obtain the optimal twitch force and a supramaximal
240 stimulation current of 600mA was used for stimulation. After a 5 min equilibration,
241 isometric tension was evaluated by 200 ms trains of pulses delivered at 10, 20, 40, 60, 80,
242 100, and 120 Hz. Length was determined with a digital microcaliper. After the
243 experimental protocol, muscles were trimmed proximal to the suture connections, excess
244 moisture was removed, and the muscle was weighed. The cross-sectional area for each
245 muscle was determined by dividing the mass of the muscle (g) by the product of its
246 length (L₀, mm) and the density of muscle (1.06 g cm⁻³) and was expressed as millimeters
247 squared (mm²). Muscle output was then expressed as specific force (N/cm²) determined
248 by dividing the tension (N) by the muscle cross-sectional area.

249 *Total RNA and qRT-PCR Gene Expression.* Total RNA was extracted from mouse EDL
250 muscles using TRIzol (Invitrogen) phenol/chloroform extraction. RNA was reverse-
251 transcribed using SuperScript IV Reverse Transcriptase and random primers (Invitrogen).

252 Reactions were incubated at 50°C for 50 minutes and at 85°C for 5 minutes. Real-time
253 PCR was performed using an ABI ViiA-7 system (Applied Biosystems). Relative
254 quantification of MyoD Family Inhibitor (MDFI), MAFbx, Murf-1, TNF α , **IL-1 β** , **IL-6**
255 mRNA levels were determined using the comparative cycles to threshold ($\Delta\Delta CT$) method
256 using FAM TaqMan gene expression assays (ThermoFisher) specific for each of these
257 genes run in complex (multiplex) with a VIC-labeled 18-S ribosomal subunit control
258 primer.

259 *Statistics.* Data are presented as a ratio of the ischemic (L) to the non-ischemic (R) limb,
260 mean \pm SEM. Force frequency and fiber typing data are presented as ischemic (L) and
261 non-ischemic (R) limbs for each strain, mean \pm SEM. Statistical analyses were carried
262 out using StatPlus:mac (v. 2009), Vassarstats (www.vassarstats.net) or Prism 6 (v. 6.0d)
263 software. *a priori* two sided t-tests were performed to examine mean differences in the
264 control limbs of the strains. All other data were compared using ANOVA with Holm-
265 Sidak multiple comparison's test or uncorrected Student's 2-tailed *t*-test. In all cases,
266 $P < 0.05$ was considered statistically significant.

267

268

269

270

271

272

273

274

275 **Supplemental References**

- 276 1. McClung JM, McCord TJ, Southerland K, Schmidt CA, Padgett ME, Ryan TE, et
277 al. Subacute limb ischemia induces skeletal muscle injury in genetically susceptible mice
278 independent of vascular density. *J Vasc Surg.* 2015.
- 279 2. Yan Z, Choi S, Liu X, Zhang M, Schageman JJ, Lee SY, et al. Highly coordinated
280 gene regulation in mouse skeletal muscle regeneration. *The Journal of biological*
281 *chemistry.* 2003;278(10):8826-36.
- 282 3. McClung JM, McCord TJ, Keum S, Johnson S, Annex BH, Marchuk DA, et al.
283 Skeletal muscle-specific genetic determinants contribute to the differential strain-
284 dependent effects of hindlimb ischemia in mice. *The American journal of pathology.*
285 2012;180(5):2156-69.
- 286 4. McClung JM, Van Gammeren D, Whidden MA, Falk DJ, Kavazis AN, Hudson
287 MB, et al. Apocynin attenuates diaphragm oxidative stress and protease activation during
288 prolonged mechanical ventilation. *Crit Care Med.* 2009;37(4):1373-9.
- 289 5. Lark DS, Reese LR, Ryan TE, Torres MJ, Smith CD, Lin CT, et al. Protein
290 Kinase A Governs Oxidative Phosphorylation Kinetics and Oxidant Emitting Potential at
291 Complex I. *Frontiers in physiology.* 2015;6:332.
- 292 6. Perry CG, Kane DA, Lin CT, Kozy R, Cathey BL, Lark DS, et al. Inhibiting
293 myosin-ATPase reveals a dynamic range of mitochondrial respiratory control in skeletal
294 muscle. *Biochem J.* 2011;437(2):215-22.
- 295 7. Spangenburg EE, Le Roith D, Ward CW, Bodine SC. A functional insulin-like
296 growth factor receptor is not necessary for load-induced skeletal muscle hypertrophy. *J*
297 *Physiol.* 2008;586(1):283-91.

298 **Supplemental Figure Legends**

299 **Supplemental Figure 1. Strain dependent myopathy with subacute hindlimb**

300 **ischemia.** Sub-acute femoral artery occlusion was performed on C57BL/6 and BALB/c

301 mice by placement of a single AC (1AC) on the proximal portion of the femoral artery,

302 immediately proximal to the epigastric arterial branch. **A.** Representative 2X and 20X

303 images of hematoxylin and eosin (H&E) stained sections of tibialis anterior (TA) muscles

304 subjected to 7 and 28 days of sub-acute ischemia. R, contralateral control limb; L,

305 ischemic limb. Arrows indicate intact muscle; Chevrons indicate regions of anucleate

306 necrotic fibers. Scale bar inlays are 1000 μ m in length(2X), and 200 μ m in length(20X).

307 **B.** Muscle regeneration was quantified from 2X H&E images by measuring the total

308 regions of interest (ROI; area) containing necrotic/anucleate myofibers and subtracting

309 from total muscle area to give a percent area of intact muscle, which is represented by

310 median and interquartile range. **C.** Total myofibers with centralized nuclei (Central.

311 Nuclei) and total myofiber number (Intact Fibers) were determined in representative 10X

312 images. Data are represented by mean \pm SEM. All data are representative of

313 N=6/strain/timepoint for each observation. * $P < 0.05$ vs. day matched C57BL/6.

314

315 **Supplemental Figure 2. Atrophy associated gene expression in ischemic hindlimbs.**

316 Sub-acute femoral artery occlusion was performed on C57BL/6 and BALB/c mice by

317 placement of a single AC (1AC) on the proximal portion of the femoral artery. QRT-PCR

318 was utilized to determine extensor digitorum longus (EDL) mRNA expression of MAFbx

319 (**A**, muscle atrophy F-box), MDFI (**B**, MyoD family inhibitor 1), and MuRF-1 (**C**, muscle

320 ring finger protein-1). Data are representative of corrected values for ribosomal subunit

321 18S mRNA and expressed as a ratio of the ischemic (L) to the non-ischemic (R) limb,
322 mean \pm SEM. N=6/strain/timepoint for each observation. * $P<0.05$ vs. day matched
323 C57BL/6.

324

325 **Supplemental Figure 3 Non-myofiber tissue deposition in ischemic hindlimb muscle.**

326 Sub-acute femoral artery occlusion was performed on C57BL/6 and BALB/c mice by
327 placement of a single AC (1AC) on the proximal portion of the femoral artery. A.
328 Sections of TA muscles were stained with picosirius red dye (PR, birefringent dye) to
329 determine collagen deposition. Representative 10X images of PR taken through a
330 polarized light filter at 7 and 28 postoperative days. Arrows indicate regions containing
331 thick collagen (orange/red birefringence); Chevrons indicate regions containing thin
332 collagen (green/yellow birefringence). Scale bar inlays are 400 μ m in length. B.
333 Green/yellow hue distribution (thin collagen deposition). C. Orange/red hue distribution
334 (thick collagen deposition). D. Sections of TA muscles were immunofluorescently
335 labeled with CD31⁺ (PECAM-1⁺) for the analysis of capillary density. Scale bar inlays
336 are 200 μ m in length (E). All data are presented as the ratio of the ischemic (L) to the non-
337 ischemic (R) limb, mean \pm SEM and representative of N \geq 6/strain/time point. * $P=0.06$
338 vs. day matched C57BL/6.

339

340 **Supplemental Figure 4. Strain dependent intramuscular lipid content during**

341 **ischemia.** Sub-acute femoral artery occlusion was performed on C57BL/6 and BALB/c
342 mice by placement of a single AC (1AC) on the proximal portion of the femoral artery.
343 A. Sections of TA muscle were histologically stained with Oil Red-O to determine

344 muscle lipid content. Scale bar inlays are 400µm in length. **(B)**. **C**. Sections of TA
345 muscles were also immunofluorescently labeled with BODIPY for the determination of
346 intermuscular lipid inclusions. Scale bar inlays are 400µm in length. **(D)**. All data are
347 presented as ratio of the ischemic (L) to the non-ischemic (R) limb, mean ± SEM and
348 representative of N=6/strain/timepoint for each observation. Non-significant trend
349 observed at 28d for Oil Red-O ($p=0.09$).

350

351 **Supplemental Figure 5 Skeletal muscle innate immune response during ischemia.**

352 Sub-acute femoral artery occlusion was performed on C57BL/6 and BALB/c mice by
353 placement of a single AC (1AC) on the proximal portion of the femoral artery. Western
354 blotting was performed for qualitative observation of Mac-1 (CD11b) protein
355 abundances, with GAPDH protein blotting as a loading reference **(A,B)**. QRT-PCR was
356 utilized to determine extensor digitorum longus (EDL) mRNA expression of TNF- α **(C)**,
357 Tumor necrosis factor-alpha), IL-1 β **(D)**, Interleukin 1 beta), and IL-6 **(E)**, Interleukin 6).
358 Data are representative of corrected values for ribosomal 18S subunit mRNA and
359 expressed as a ratio of the ischemic (L) to the non-ischemic (R) limb, mean ± SEM.
360 N=6/strain/timepoint for each observation. * $P<0.05$ vs. day matched C57BL/6

361

362 **Supplemental Figure 6. Verification of myotoxin injury as non-ischemic.** Cardiotoxin

363 (CTX) was injected intramuscularly into the TA and the lateral/medial heads of the
364 gastrocnemius muscle. A sham injection of equal volume sterile saline was injected in the
365 same muscles in the contralateral control limb (R). **A**. Laser Doppler perfusion imaging
366 (LDPI) was performed and regionally analyzed (thigh, paw, and whole limb). **B**. Tissue

367 oxygen saturation (SO₂) was measured via white light reflectance spectroscopy over the
368 tibialis anterior and Gastrocnemius muscles after injury. Data are representative of the
369 ratio of the ischemic (L) to the non-ischemic (R) limb, mean ± SEM. All data are
370 representative of N=6/strain/timepoint for each observation. * *P*<0.05 vs. day matched
371 C57BL/6.

372

373 **Supplemental Figure 7. Distribution of myotoxic injury to the anterior limb**
374 **compartment.** Cardiotoxin (CTX) was injected intramuscularly into the TA and the
375 lateral/medial heads of the gastrocnemius muscle. Representative 20X images of
376 hematoxylin and eosin (H&E) stained sections of tibialis anterior (TA) and extensor
377 digitorum longus (EDL) muscles 24hrs after CTX injection into the TA. R, contralateral
378 control limb; L, ischemic limb.

379

380 **Supplemental Figure 8. Non-myofiber tissue deposition in non-ischemic**
381 **regenerating muscle.** Non-ischemic muscle regeneration was induced by cardiotoxin
382 (CTX) injection. **A.** Sections of TA muscles were stained with picosirius red dye (PR,
383 birefringent dye) to determine collagen deposition. Representative 10X images of PR
384 taken through a polarized light filter at 7 and 28 postoperative days. Arrows indicate
385 regions containing thick collagen (orange/red birefringence); Chevrons indicate regions
386 containing thin collagen (green/yellow birefringence). Scale bar inlays are 400µm in
387 length **B.** Green/yellow hue distribution (thin collagen deposition). **C.** Orange/red hue
388 distribution (thick collagen deposition). **D.** Sections of TA muscle were
389 immunofluorescently labeled with CD31⁺ (PECAM-1⁺) for the analysis of capillary

390 density (**E**). Scale bar inlays are 200µm in length. All data are presented as ratio of the
391 ischemic (L) to the non-ischemic (R) limb, mean ± SEM and representative of
392 N≥6/strain/time point. * $P < 0.05$ vs. day matched C57BL/6, or indicated non-significant
393 trend vs. day matched C57BL/6 Thin Collagen ($p = 0.07$).

394

395 **Supplemental Figure 9. Strain dependent intramuscular lipid content during non-**
396 **ischemic injury.** Cardiotoxin (CTX) was injected intramuscularly into the TA and the
397 lateral/medial heads of the gastrocnemius muscle. **A.** Sections of TA muscle were
398 histologically stained with Oil Red-O to determine muscle lipid content. Scale bar inlays
399 are 400µm in length (**B**). **C.** Sections of TA muscles were also fluorescently labeled with
400 BODIPY for the determination of intermuscular lipid inclusions. Scale bar inlays are
401 400µm in length (**D**). All data are presented as ratio of the ischemic (L) to the non-
402 ischemic (R) limb, mean ± SEM and representative of N=6/strain/timepoint for each
403 observation. * Non-significant trend observed at 7d for Oil Red-O ($p = 0.07$).

404

405

406

407

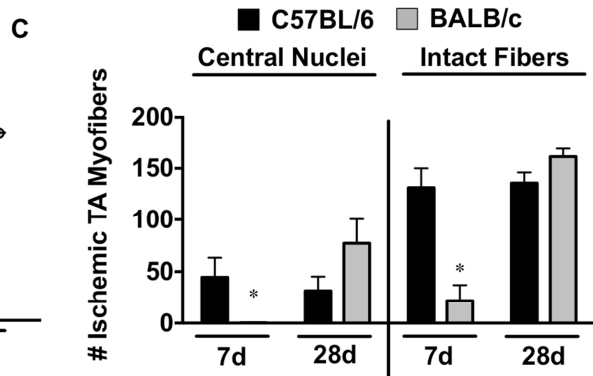
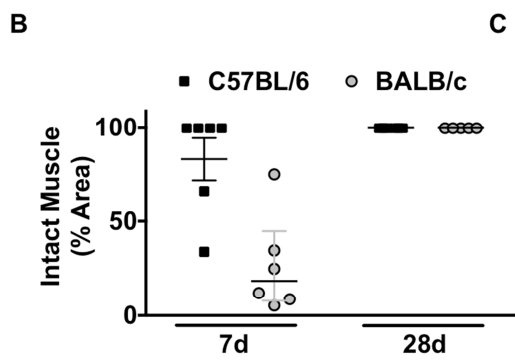
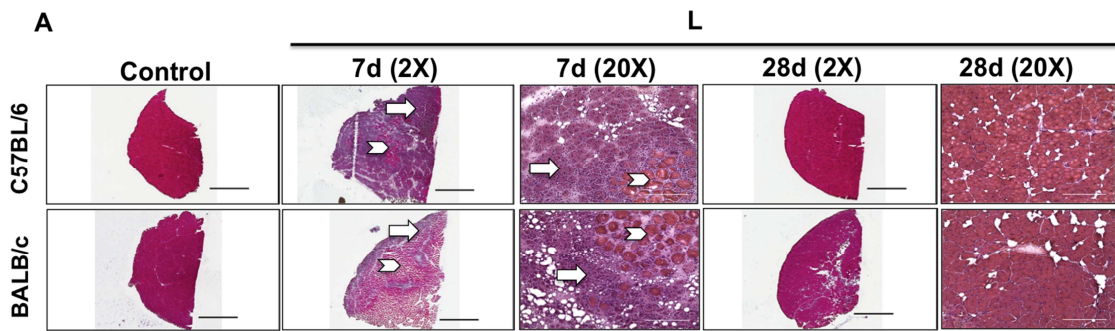
408

409

410

411

412 Supplemental Figure 1



413

414

415

416

417

418

419

420

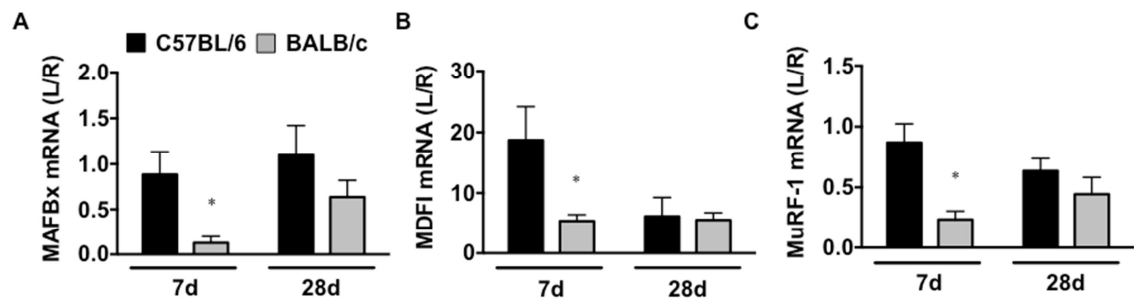
421

422

423

424

425 **Supplemental Figure 2**



426

427

428

429

430

431

432

433

434

435

436

437

438

439

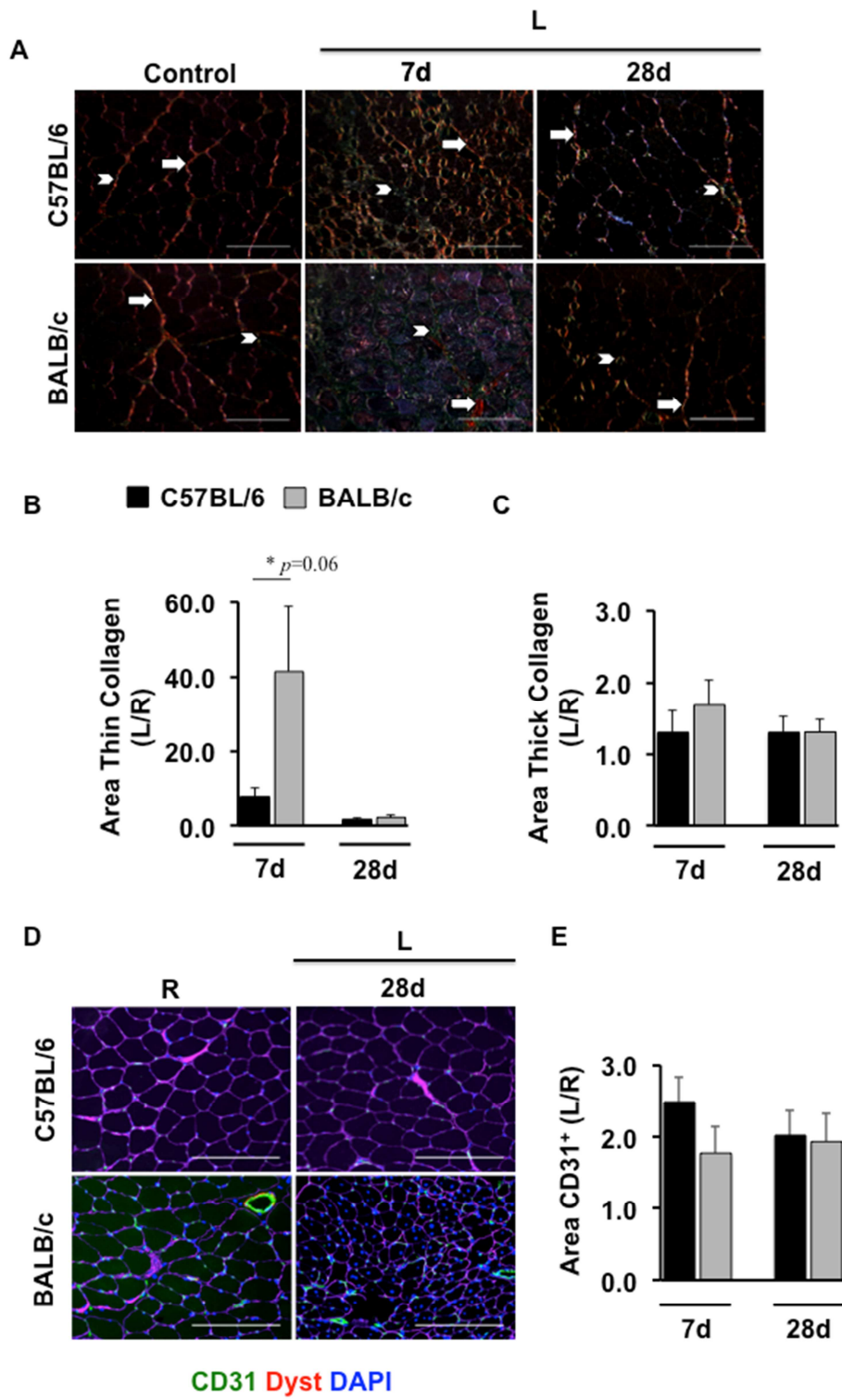
440

441

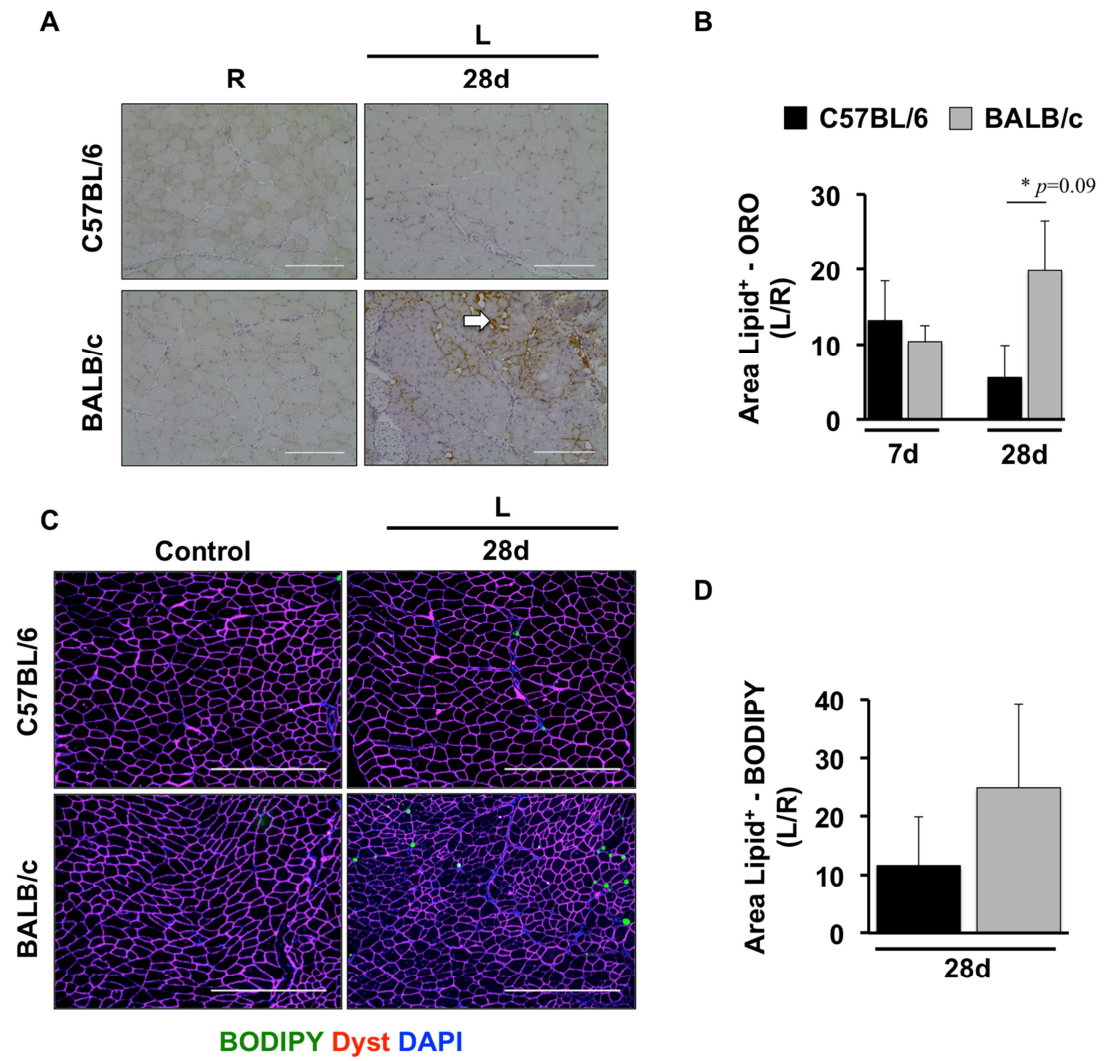
442

443

444



447 Supplemental Figure 4



448

449

450

451

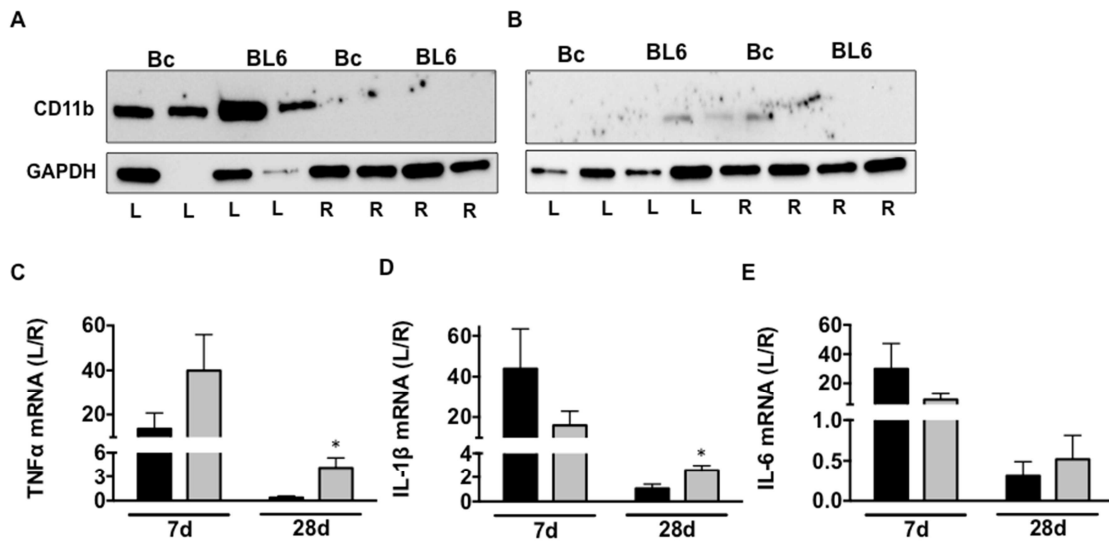
452

453

454

455

456 **Supplemental Figure 5**



457

458

459

460

461

462

463

464

465

466

467

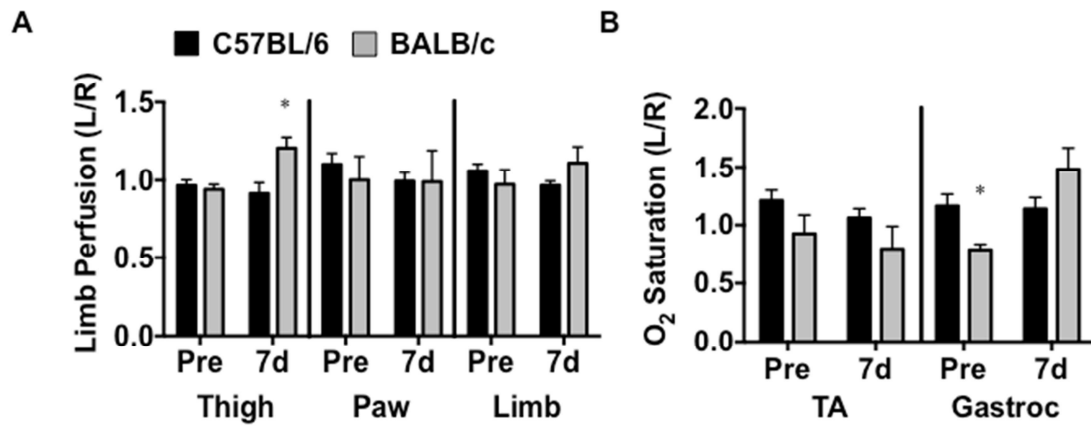
468

469

470

471

472 Supplemental Figure 6



473

474

475

476

477

478

479

480

481

482

483

484

485

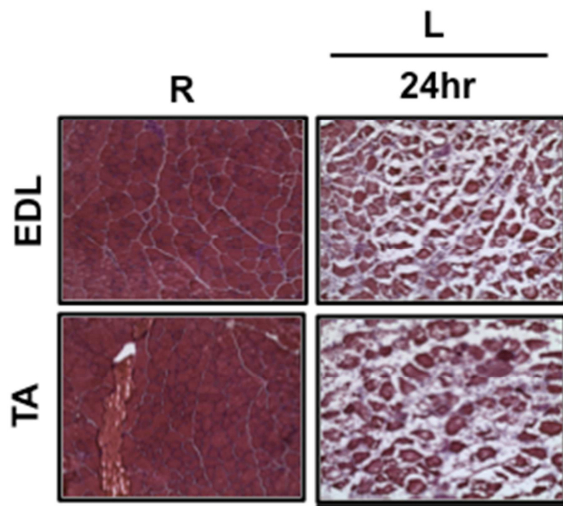
486

487

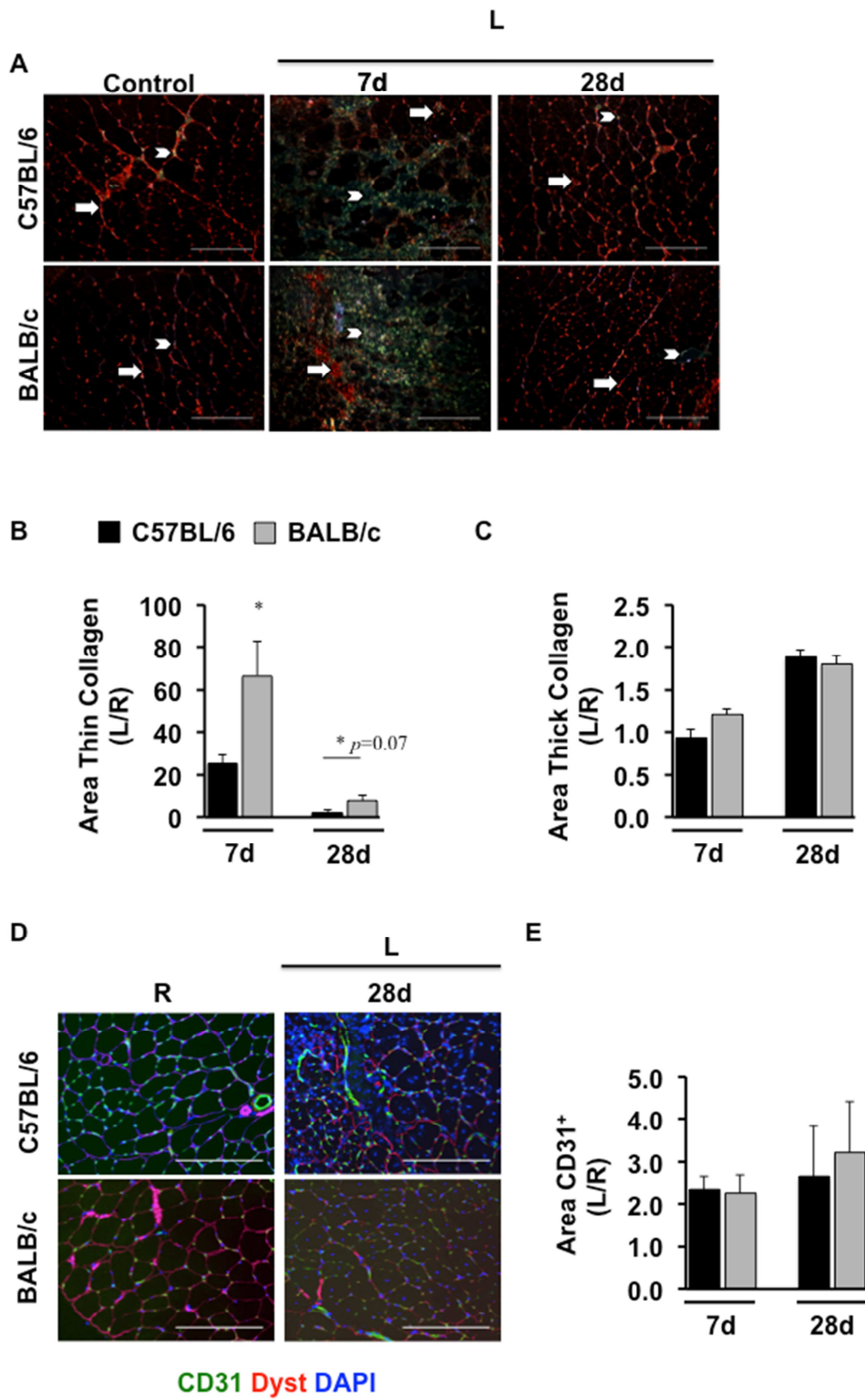
488

489

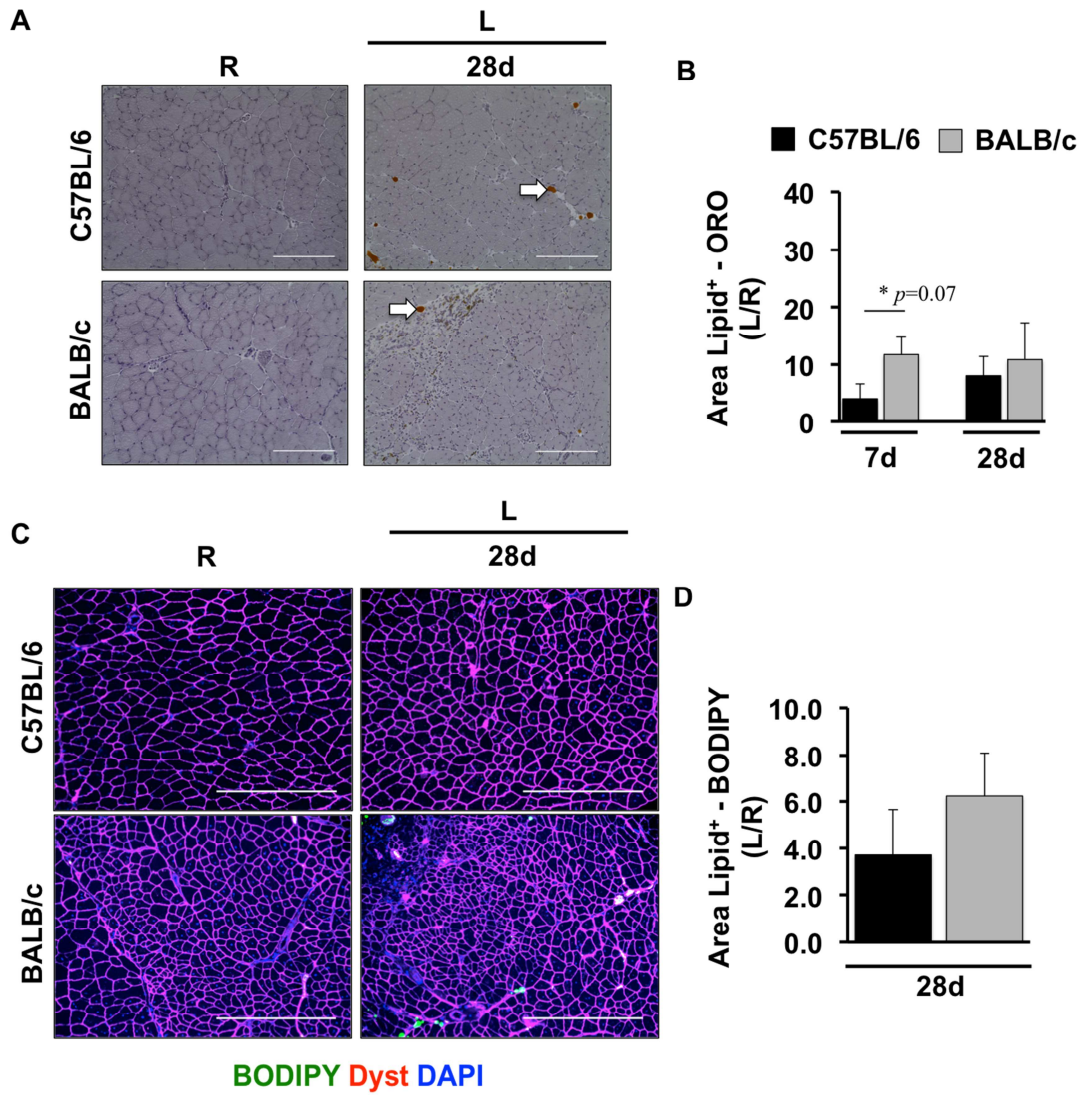
490 **Supplemental Figure 7**



491
492
493
494
495
496
497
498
499
500
501
502
503
504
505
506



509 Supplemental Figure 9



510